Reproduction and Breeding 3 (2023) 208–218

Contents lists available at ScienceDirect

Reproduction and Breeding

journal homepage: www.keaipublishing.com/en/journals/reproduction-and-breeding

Tumor necrosis factor α1 (TNFα1) administration can disrupt barrier function and attenuate redox defense in midgut of red crucian carp (*Carassius auratus* red var)

Jin-Fang Huang [a], Ning-Xia Xiong [a,b], Shi-Yun Li [a], Ke-Xin Li [a], Jie Ou [a], Fei Wang [a], Sheng-Wei Luo [a,*]

[a] State Key Laboratory of Developmental Biology of Freshwater Fish, College of Life Science, Hunan Normal University, Changsha, 410081, PR China
[b] Department of Aquatic Animal Medicine, College of Fisheries, Huazhong Agricultural University, Wuhan, 430070, PR China

ARTICLE INFO

Keywords:
Crucian carp
Cytokines
Gene expression
Gut immunity

ABSTRACT

TNFα belongs to superfamily of tumor necrosis factor that can exert the pleiotropic effort in a large quantity of biological processes, including immune homeostasis, intracellular modulation and etiopathogenesis, but its regulatory role in mucosal immune regulation of fish is unclear. Currently, this study aimed to evaluate the immunoregulatory function of TNFα1 on gut barrier in teleost fish. In this study, TNFα1 sequences were identified from red crucian carp (RCC, *Carassius auratus* red var). The high-level expression of RCC-TNFα1 mRNA was detected in gill among all the isolated samples. Then, RCC-TNFα1 expression increased dramatically in immune-related tissues after *A. hydrophila* infection and in cultured fish cells after lipopolysaccharide (LPS) treatment. RCC-TNFα1 fusion protein was generated and purified *in vitro*. RCC receiving RCC-TNFα1 perfusion showed an increased levels of villi fusion and edema in injured midgut with the fuzzy appearance. In addition, The mRNA expressions of tight junction (TJ) genes, mucin genes and redox sensitive genes decreased sharply in TNFα1-treated midgut in comparison with those of the control ($P < 0.05$), whereas the expression levels of apoptotic genes involved in caspase signals and unfolded protein response (UPR) attained the dramatic increase. These results demonstrated that RCC-TNFα1 stimulation could impair midgut structural integrity and immune function by induction of antioxidant collapse and apoptotic activation.

1. Introduction

A wide range of ambient stressors can directly disturb normal physiological processes in animals [1]. Previous findings suggest that biotic or abiotic stressors may exhibit an immunosuppressive effect on fish, rendering fish more susceptible to pathogenic invasion [2]. In addition, abuse of antibiotics administration or release of heavy metals may dramatically alter the natural population of microbes and then facilitate superbug enrichment in aqueous surroundings [3]. Whist invading pathogens succeed in breach of mucosal barriers, they can immediately exacerbate infectious diseases and orchestrate innate immune response in fish during pathogen-induced inflammation [4]. Although immunoprophylactic treatments can significantly boost fish immunity and then restrict dispersal of infectious diseases during aquaculture processes, pollutant bioaccumulation can dramatically alter the microbe community in water environment, then facilitating the emerging pathogenic bacteria with multiple resistance and virulence [5]. Crucian carp (*Carassius auratus*) is an important farmed fish species in China, but its farming process suffers from pathogenic infection [6]. As known pathogenic bacteria, *Aeromonas hydrophila* can increase fish morbidity by generating toxins [7]. Our previous studies indicated that gut infection with *A. hydrophila* can disrupt epithelial permeability in midgut, increase bacterial burdens as well as dysregulate immune response in gut-liver axis of RCC [8].

Fish possess a variety of immune-related properties such as pathogen recognition receptors (PRRs) and complement cascades, which can serve as the first line of immune defense against pathogenic infection [9]. Gut-associated lymphoid tissue (GALT) is playing an important role in mucosal immune defense and pathogenic elimination in fish [10], whereas gut mucosal surface acting as biophysical barrier can promote mucus secretion, increase immune surveillance as well as establish a microenvironment in gut-liver axis maintained by a reciprocal

* Corresponding author. College of Life Science, Hunan Normal University, Changsha, 410081, PR China.
E-mail addresses: swluo@hunnu.edu.cn, swluo1@163.com (S.-W. Luo).

https://doi.org/10.1016/j.repbre.2023.11.001
Received 17 September 2023; Received in revised form 26 October 2023; Accepted 13 November 2023

interaction between gut, gut flora and liver [11,12]. Recent findings demonstrate that activation of immune-related signals, including pattern recognition, cytokine production as well as immune cell signals, are involved in synergistic effect on immune regulation of gut-liver axis in fish after pathogenic infection [13,14]. Among known immune regulators, TNFα is a glycopeptide hormone that can exert a pleiotropic role in immune activation, inflammatory response and apoptotic processes [15]. Although TNFα function has been extensively studied in mammals, fish contain multiple isoforms of TNFα gene [16]. Some studies focused on gene structure and immune regulation of TNFα in large yellow croaker [17], zebrafish and medaka [18], but the immunoregulatory function of TNFα1 on gut mucosal barrier in RCC was unclear.

In this study, the aims were to characterize architectures of TNFα1 in RCC. Then, the expression profiles of TNFα1 in immune-related tissues or cultured cell lines were investigated. After that, TNFα1 fusion protein was generated *in vitro* and then its immunoregulatory effect on gut mucosal barrier function was studied, providing a new insight into the regulatory function of TNFα1 in RCC.

2. Materials and methods

2.1. Animals

Healthy RCCs were collected from earthen ponds in a fishing base (Changsha, China). The water temperature ranged from 19 °C to 26 °C. RCCs (approximately 18.91 ± 1.25 g) were acclimatized in aquarium for two weeks and fed with commercial diet twice daily till 24 h before challenge experiment. Water quality was maintained to avoid pathogenic contamination by removing the excess of dietary feed and fish feces daily.

2.2. Infection with A. hydrophila

A. hydrophila was cultured in Luria-Bertani (LB) medium at 28 °C for 24 h, centrifuged at 12000×*g* and resuspended in 1 × PBS (pH 7.3) before challenge experiment [19]. Intraperitoneal injection of *A. hydrophila* (1×10^7 CFU ml^{-1}) served as *A. hydrophila* infection group, while equivalent volume of sterile PBS injection was used as control group. Tissues were isolated at 0, 6, 12, 24, 36 and 48 h post-injection, immediately frozen in liquid nitrogen and preserved in −80 °C. Each group contained three biological replicates, respectively.

2.3. Cell culture and LPS stimulation

RCC fibroblast cells (RCCFCs) were cultured in DMEM medium at 26 °C with a humidified atmosphere of 5 % CO_2 as described previously [20]. Then, RCCFCs were seeded into 6-well plates at 80 % confluence for 24 h. Then, cultured medium was replaced with fresh medium containing 500 ng/mL of LPS (*Escherichia coli* O111:B4, Sigma, USA) [21]. Cells were harvested at 0, 6, 12, 24, 36 and 48 h post-treatment, frozen in liquid nitrogen and preserved in −80 °C.

2.4. Gene cloning, bioinformatics analysis and plasmid construction

Open reading frame (ORF) sequences of RCC-TNFα1 were cloned by using the primers TNFα1-F: ATGATGGATCTTGAGAGTCAGCT and TNFα1-R: TCATAAAGCAAACACCCCGAA. Domain architectures were analyzed by NCBI blast, SignalP 5.0 server, TMHMM 2.0 server and phyre2 program, while phylogenetic analysis was constructed by using MEGA 6.0. Enzyme cleavage sites were added to the ORF sequence by using primers pet-TNFα1-F: CCGGAATTCATGCTCAACAAGTCTCAGAA and pet-TNFα1-R: CCGCTCGAGTTAATGATGATGATGATGATGTAAAGCAAACACCCCGAAGA. ORF sequence was ligated to pET32α plasmid and then transformed into *Escherichia coli* BL21 (DE3) competent cells for fusion protein production. Positive bacterial clone was subjected for sequencing confirmation (Tsingke, China).

Table 1
The primer sequences used in this study.

Primer names	Sequence direction (5' → 3')	Use	AN of original sequence
RT-TNFα1-F	TGTGGGGTCCTGCTGGC	qPCR	OR712226
RT-TNFα1-R	TTCCTGATTGTTCTGAGACTTGTTG	qPCR	
RT-FADD-F	TTGTGCCAAGAAGAAGTCGG	qPCR	OR712228
RT-FADD –R	TGTTTTCGCAGGAGTTCAGTG	qPCR	
RT-CASP7-F	CTAAGCCACGGCGAGGA	qPCR	OR712229
RT- CASP7-R	CGGAACCCCGACAAGC	qPCR	
RT-CASP3-F	AGATGCTGCTGAGGTCGGG	qPCR	OR712230
RT-CASP3-R	GGTCACCACGGGCAACTG	qPCR	
RT-CASP8-F	TGTGAATCTTCCAAAGGCAAA	qPCR	OR712231
RT-CASP8-R	CTGTATCCGCAACAACCGAG	qPCR	
RT-HSP70-F	ACGAGGCAGTGGCTTATGG	qPCR	OR712232
RT-HSP70-R	GGGTCTGTTTGGTGGGGAT	qPCR	
RT-HSP90α-F	AGCAGCCGATGATGGA	qPCR	OR712233
RT-HSP90α-R	GGATTTGGCGATGGTTC	qPCR	
RT-HSP90β-F	TGGGATTGGGGATTGATGA	qPCR	OR712234
RT-HSP90β-R	CCTTCCAGAGGTGGGATTTC	qPCR	
RT-ATF4-F	CCTGGACTCACTTCCGTTCG	qPCR	OR712235
RT-ATF4-R	GCTGCCGTTTTGTTCTGCT	qPCR	
RT-ATF6-F	TCTGTGATGAAAGCAACCGC	qPCR	OR712236
RT-ATF6-R	CAGGGGCAGCAGGAAATG	qPCR	
RT-IRE1-F	AGCGGCAAGCAAACATTCT	qPCR	OR712237
RT-IRE1-R	CCACCATCCGTCCTCCTCT	qPCR	
RT-PDIA3-F	CTGAGCCTGTTCCAGAGTCCA	qPCR	OR712238
RT- PDIA3-R	TCCAGAGGGCACAAAGTAAATG	qPCR	
RT-XBP1-F	TCCACTTTGACCACATCTACACC	qPCR	OR727861
RT-XBP1-R	TTCATCTTTGACGGACACCATT	qPCR	
RT-ZO-1-F	TGCCCAGAGGTGAAGAGGTC	qPCR	OR727864
RT- ZO-1-R	GCCCAGTTTGCCGTTGTAA	qPCR	
RT-occludin –F	GTTGCCCATCCGTAGTTCAGT	qPCR	OR727865
RT-occludin –R	CTTCAGCCAGACGCTTGTTG	qPCR	
RT-claudin-3-F	GTCAATGGGAATGGAGATGGG	qPCR	OR727866
RT-claudin-3-R	AAGCCTGAAGGTCTTGCGATA	qPCR	
RT-claudin-6-F	GACCATCGCTGTTCCAAGA	qPCR	OR727867
RT-claudin-6-R	ATTCCATCCACAAGCCCTC	qPCR	
RT-claudin-9-F	GGCAAACACGGGTCTTCAG	qPCR	OR727868
RT-claudin-9-R	CGGTGCGGCGACATTC	qPCR	
RT-MUC2-F	CCTGACATTTTGTGGTGGAGA	qPCR	OR727869
RT-MUC2-R	CTGTGCGATTACTTGAGCGAG	qPCR	
RT-MUC13-F	TGCCACATCAGTTTCAGTTGC	qPCR	OR727870
RT-MUC13-R	TTCACCCACCGCCATTTC	qPCR	
RT-MUC7-F	AGACCAAAGCCCACGCAG	qPCR	OR727871
RT-MUC7-R	ACACCAGTCCAGCCAGCAG	qPCR	
RT-OXR1-F	CATCAGGCAGCATTAGAGGC	qPCR	OR727872
RT-OXR1-R	TGGAGGGGATTTTAGGTTTTG	qPCR	
RT-TrxR-F	TCCTGGGGTCTGGGTGG	qPCR	OR731261
RT-TrxR-R	CAGCCGAACTTGCGTGC	qPCR	
RT-SOD1-F	GGACCAACGGATAGCGACA	qPCR	OR727873
RT- SOD1-R	CCAGGCGACTTCCAGCG	qPCR	

2.5. Prokaryotic expression, purification and western blotting of TNFα1

Generation and purification of fusion proteins were performed as described previously [22]. The above *E. coli* BL21 clones inserted with corrected plasmids were cultured until OD_{600} value reached about 0.6, then 1 mM IPTG was added for another 4 h incubation. Pellets were harvested for sonication treatment, dissolved in urea-containing buffer. After centrifugation, supernatant proteins were purified by using

Ni-NTA resins. After dialysis, purified TNFα1 fusion proteins were validated by western blotting [23]. The purified TNFα1 fusion proteins were loaded on SDS-PAGE gel, separated electrophoretically and transferred to PVDF membranes. After incubation with blocking buffer, membranes were reacted with 1:2000 diluted His-tag antibody and enzyme-conjugated secondary antibody, respectively. Finally, PVDF membranes were developed and visualized.

2.6. Gut perfusion with TNFα1 fusion protein

Gut perfusion assay was performed as described previously [24–26]. Briefly, fish were anally intubated with TNFα1 fusion protein (0.15 mg/per fish) by using a gavage needle inserted into a depth of approximately 3 cm, while equivalent per gram of pET32α tag perfusion was used as control group, respectively. Tissues were isolated at 48 h post-perfusion, then immediately frozen in liquid nitrogen and preserved in −80 °C. Each group contained three biological replicates, respectively.

2.7. RNA isolation, cDNA synthesis and qRT-PCR assay

Total RNA was extracted from isolated tissues and harvested cells by using HiPure Total RNA Mini Kit (Magen, China). Following quality check, 1000 ng of purified total RNA was used for cDNA synthesis by using MonScript™ RT III All-in-One Mix with dsNase (Monad, China). Relative expressions of TNFα1, Fas-associating protein with a novel death domain (FADD), caspase 7 (CASP7), caspase 3 (CASP3), caspase 8 (CASP8), heat shot protein 70 (HSP70), heat shot protein 90α (HSP90α), heat shot protein 90β ((HSP90β), activating transcription factor 4 (ATF4), activating transcription factor 6 (ATF6), Inosital-requiring enzyme 1 (IRE1), protein disulfide isomerase family A, member 3 (PDIA3), X-box binding protein 1 (XBP1), zonula occludens-1 (ZO-1), occludin, claudin-1, claudin-3, claudin-6, and claudin-9, oxidation resistance 1 (OXR1), thioredoxin reductase (TrxR), CuZnSOD (SOD1), mucin 2 (MUC2), mucin 7 (MUC7) and mucin 13 (MUC13) were investigated by qRT-PCR assay [27]. In brief, qRT-PCR assay was performed by using PowerUp SYBR Green Master Mix (Applied Biosystems, USA). At the end of qRT-PCR assay, melting curve analysis was implemented to confirm credibility of each qRT-PCR result. The primers used in this study were shown in Table 1. 18S rRNA was amplified by using primers RT-18S–F: CGGAGGTTCGAAGACGATCA and RT-18S–R: GAGGTTTCCCGTGTTGAGTC, which was used as internal control to normalize the results. Efficiency of the primers used in this study was over 95 %, and their product sizes ranged from 100 bp to 300 bp. Primer specificity was confirmed and each sample was analyzed in triplicate to certify the repetitiveness and credibility of experimental results. Accession numbers (AN) of the original sequences were presented in Table 1. qRT-PCR results were measured by using Applied Biosystems QuantStudio 5 Real-Time PCR System with $2^{-\triangle\triangle Ct}$ methods.

```
ATG ATG GAT CTA GAG AGT CAG CTT GTT GAA GAA GGG GGA TTG CTG  47
 M   M   D   L   E   S   Q   L   V   E   E   G   G   L   L  15
CCC TCA CGG CAG GTG ACG GTG TCG AGG AGG ACG TCC GGT GTC TGG  92
 P   S   R   Q   V   T   V   S   R   R   T   S   G   V   W  30
CGG GTG TGT GGG GTC CTG CTG GCT GTG GCC CTG TGT GCC GCC GCC 137
 R   V   C   G   V   L   L   A   V   A   L   C   A   A   A  45
GCT GTC TGC TTC ACG CTC AAC AAG TCT CAG AAC AAT CAG GAA GGA 182
 A   V   C   F   T   L   N   K   S   Q   N   N   Q   E   G  60
GGA AAT GCG CTG AGG CTC ACA TTA AGA GAT CGT CTT TCA AAG CAA 227
 G   N   A   L   R   L   T   L   R   D   R   L   S   K   Q  75
AAC GTC ACT TCC AAG GCT GCC ATC CAT TTA ACA GGT GCG TAT GAA 272
 N   V   T   S   K   A   A   I   H   L   T   G   A   Y   E  90
CCT AAA GTG TCC AAA GAC ACC CTT TAC TGG AGA AAG GAC CAG GAC 317
 P   K   V   S   K   D   T   L   Y   W   R   K   D   Q   D 105
CAG GCT TTC ACT TCA GGC GGC TTG AAA TTA GCG GGA AGG GGG ATC 362
 Q   A   F   T   S   G   G   L   K   L   A   G   R   G   I 120
ATC ATT CCT ACG GAT GGC ATT TAC TTC GTC TAC AGT CAG GTG TCT 407
 I   I   P   T   D   G   I   Y   F   V   Y   S   Q   V   S 135
TTC CAC ATC AGA TGC AAG ACT GAC ATT CCT GAG GAC CAC GAT GTT 452
 F   H   I   R   C   K   T   D   I   P   E   D   H   D   V 150
GTG CAA ATG AGC CAC ATA GTG TTC CGC TAC TCT GAT TCC TAT GGC 497
 V   Q   M   S   H   I   V   F   R   Y   S   D   S   Y   G 165
AGC TAC AAG CCA CTT TTC AGC GCA ATC CGC TCG GCC TGC GAG CAG 542
 S   Y   K   P   L   F   S   A   I   R   S   A   C   E   Q 180
GCG ACA GAC TCT GAC GAT CTG TGG TAC AAC ACG ATT TAT CTC GGT 587
 A   T   D   S   D   D   L   W   Y   N   T   I   Y   L   G 195
GCG GCC TTC AGC CTG CGA GCC GAA GAC AGG CTG TGC ACT AAT ACG 632
 A   A   F   S   L   R   A   E   D   R   L   C   T   N   T 210
ACT ATA GCA CTC CTG CCT CGC GTC GAA AGC GAC AAC GGA AAG ACC 677
 T   I   A   L   L   P   R   V   E   S   D   N   G   K   T 225
TTC TTT GGG GTG TTT GCG TTA TGA                            704
 F   F   G   V   F   A   L END                             233
```

Fig. 1. Nucleotide sequence and deduced amino acid sequence of RCC-TNFα1.

2.8. Histological analysis

The above anally intubated midgut samples were fixed in Bouin solution, dehydrated in ethanol, clarified in xylene, and embedded in paraffin wax. Then, samples were sectioned (approximately 5 μm thick) and stained by using a periodic acid-schiff (PAS) staining kit [28]. Prepared slides were observed by using a light microscope with 200 × magnification. The average changes of goblet cell (GC) numbers and villus length-to-width (L/W) ratios were calculated. The experiment was repeated in triplicate.

2.9. Detection of biochemistry change

2.9.1. Catalase (CAT) activity

CAT activities in midgut were measured at OD_{405} absorbance by using a CAT activity kit (Nanjing Jiancheng Bioengineering Institute, China). Results were given in units of CAT activity per milligram of protein, where 1 U of CAT is defined as the amount of enzyme decomposing 1 μmol H_2O_2 per second. The experiment was repeated in triplicate.

2.9.2. Glutathione peroxidase (GPx) activity

GPx activities in midgut were observed at OD_{340} absorbance by using a GPx activity kit (Beyotime Biotechnology, China). Results were shown as U GPx activity per milligram of protein. The experiment was repeated in triplicate.

2.9.3. Total superoxide dismutase (SOD) activity

Total SOD activity in midgut were detected at OD_{560} absorbance by using a total SOD activity kit (Beyotime Biotechnology, Shanghai, China). Results were given in units of SOD activity per milligram of protein, where 1 U of SOD is defined as the amount of enzyme producing 50 % inhibition of SOD. The experiment was repeated in triplicate.

2.9.4. Succinate dehydrogenase (SDH) activity

SDH activity in midgut was detected at OD_{600} absorbance by using a SDH activity kit (Nanjing Jiancheng Bioengineering institute, China). Following triplicate measurements, mean values were shown as U SDH per milligram of protein.

2.9.5. NADPH/$NADP^+$ ratio

NADPH/$NADP^+$ contents in midgut were determined by using NADPH/$NADP^+$ assay kit (Beyotime Biotechnology, Shanghai, China). Then, NADPH/$NADP^+$ ratios were calculated as: [NADPH]/[$NADP^+$] = [NADPH]/([NADP total]-[NADPH]). The experiment was repeated in triplicate.

2.9.6. Determination of relative reactive oxygen species (ROS) production

ROS levels in supernatants of 10 % midgut homogenates were measured by DCFH-DA probe. After triplicate repeats, ROS contents were calculated with absorbance changes at excitation/emission wavelength of $OD_{480/520}$ nm.

2.9.7. Malondialdehyde (MDA) amounts

Free MDA and lipid hydroperoxides can be determined by thiobarbituric acid (TBA) method. According to protocols of lipid

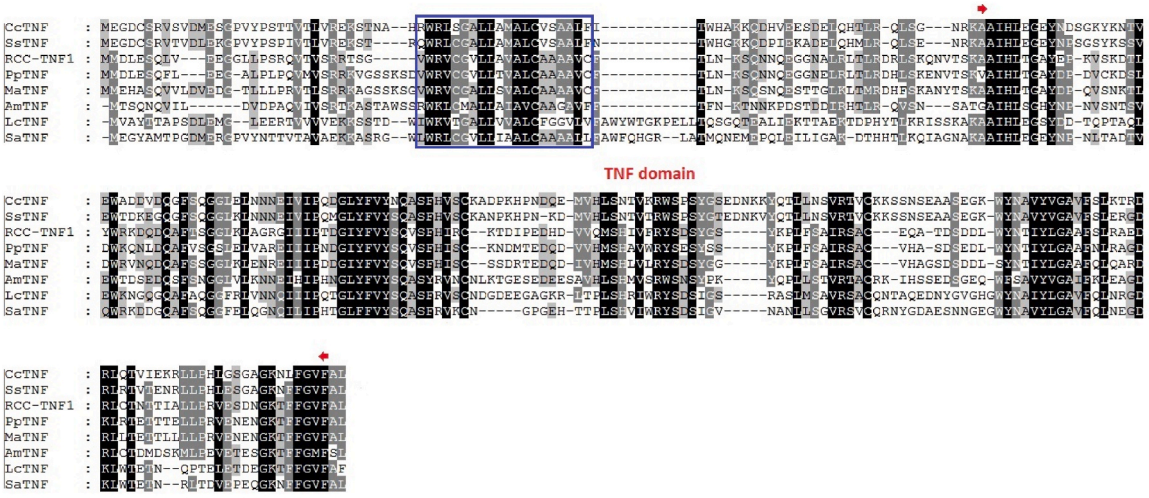

A

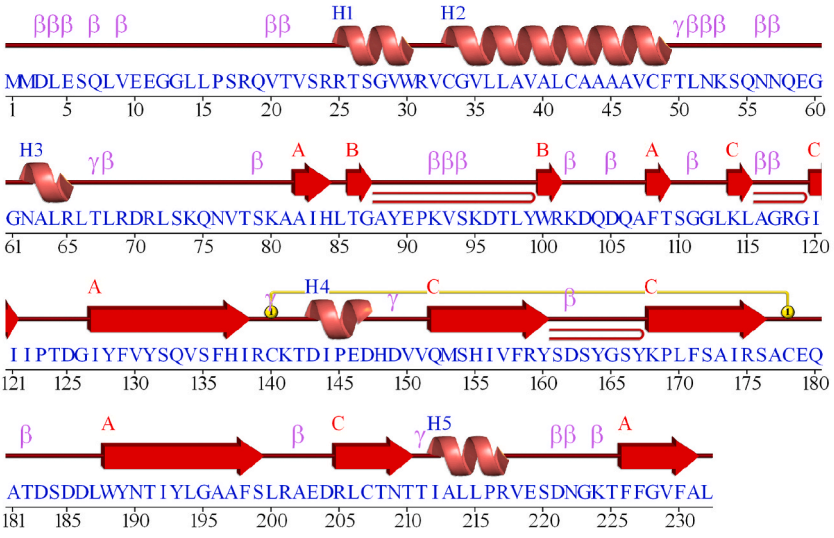

B

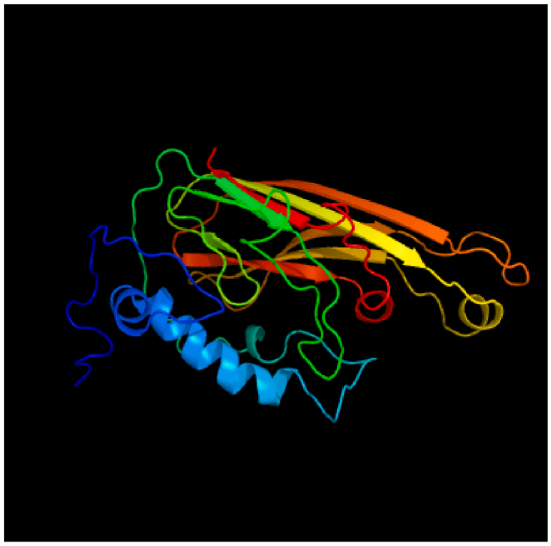

C

(caption on next page)

Fig. 2. Bioinformatics analysis of RCC-TNFα1. (A) Alignment analysis of RCC-TNFα1 with other TNFα sequences. CcTNF, *Coregonus clupeaformis* TNFα, XP_041757942.2; AmTNF, *Astyanax mexicanus* TNFα, KAG9279623.1; SaTNF, *Salvelinus alpinus* TNFα, XP_023844956.1; SsTNF, *Salmo salar* TNFα, NP_001117089.1; PpTNF, *Percocypris pingi* TNFα, AIN25992.1; LcTNF, *Larimichthys crocea* TNFα, NP_001290314.1; MaTNF, *Megalobrama amblycephala* TNFα, ANA78340.1. The shared residues represented the similar regions between the different species and the conservative degree was distinguished from light to dark. TNF domain was indicated by arrow and transmembrane region was circled by blue box. (B) Secondary structure prediction of RCC-TNFα1. : Helix strand, Helices labeled: H1, H2, …and strands by their sheets A, B, …; β: beta turn; γ: gamma turn; : beta hairpin; : disulphide bond. (C) Tertiary structure prediction. Structures were colored by rainbow from N to C terminus.

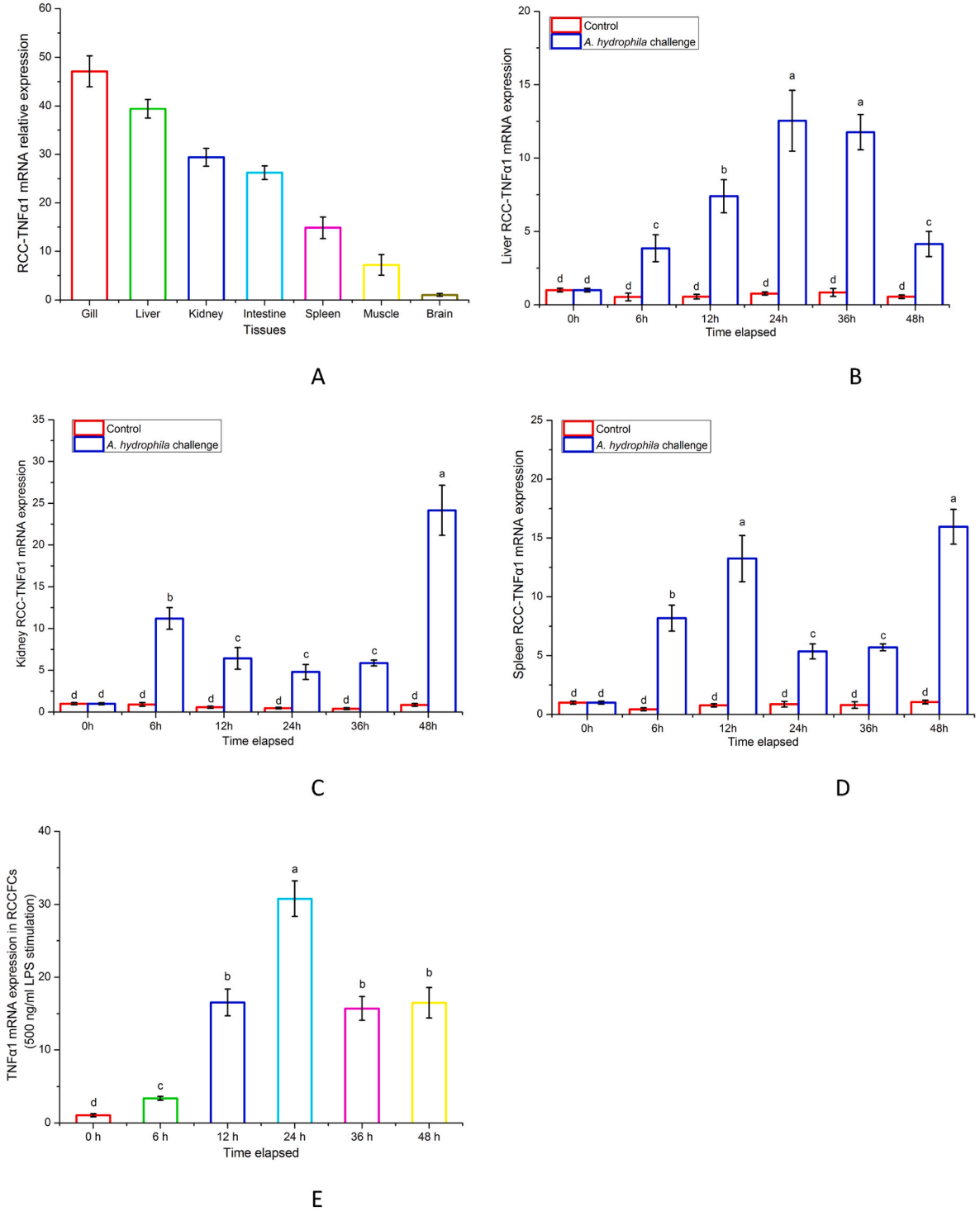

Fig. 3. Gene expression levels of RCC-TNFα1. (A) Tissue-specific expressions determined by qRT-PCR assay. (B–D) Expressions of RCC-TNFα1 were detected in liver, kidney and spleen at 0, 6, 12, 24, 36 and 48 h post-challenge. (E) Expression levels of TNFα1 in RCCFCs subjected to LPS exposure. The calculated data (mean ± SD) with different letters were significantly different ($P < 0.05$) among the groups. The experiments were performed in triplicate.

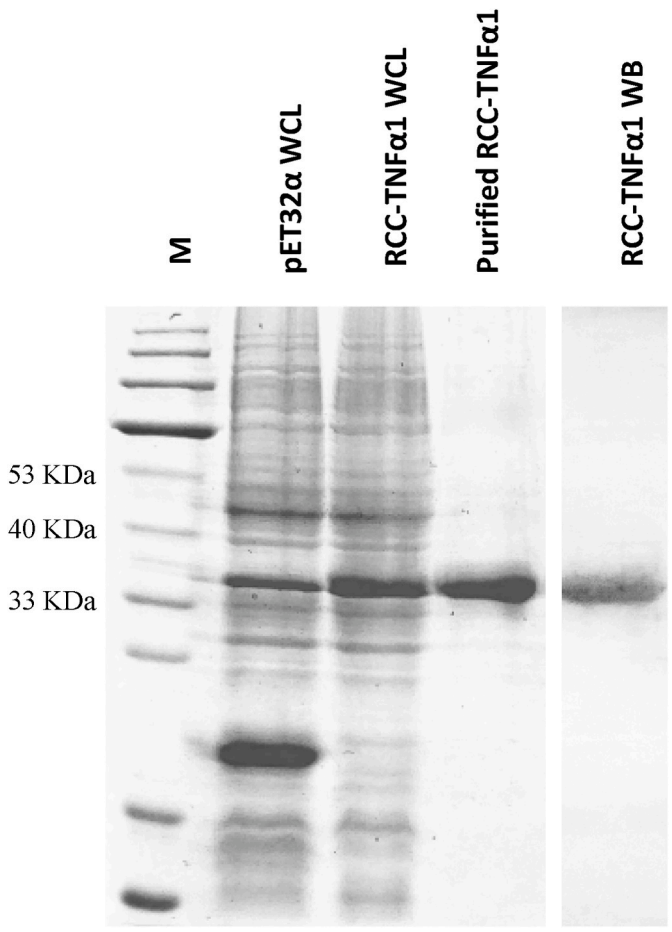

Fig. 4. Generation and validation of TNFα1 fusion proteins. Lane M: protein molecular standard; Lane pET32α WCL: total protein was isolated from lysis of pET32α-BL21 after IPTG induction; Lane RCC-TNFα1 WCL: total protein was isolated from lysis of pET32α-RCC-TNFα1-BL21 after IPTG induction; Lane purified RCC-TNFα1: RCC-TNFα1 fusion protein was purified by using Ni-NTA; Lane RCC-TNFα1 WB: purified fusion protein was identified by using anti-His tag antibody.

peroxidation MDA assay kit (Beyotime Biotechnology, Shanghai, China), midgut MDA amount was measured. The concentration of MDA was expressed as micromole MDA per milligram of protein. The experiment was repeated in triplicate.

2.9.8. Diamine oxidase (DAO) activity

DAO activity in midgut was measured by using a DAO assay kit (Solarbio, China). After triplicate measurements, DAO activity was calculated with absorbance changes at OD_{500} nm.

2.10. Statistical analyses

SPSS program was used for data calculation, which is subjected to one-way ANOVA. If the analytical levels reach less-than 0.05 P-value, results were statistically significant.

3. Results

3.1. Characterization of TNFα1 sequences

The nucleotide and deduced amino acid sequences of RCC-TNFα1 were shown in Fig. 1. The ORF sequence of RCC-TNFα1 encoded a polypeptide of 232 amino acid residues with an estimated molecular mass of 25.71 kDa and a predicted isoelectronic point of 7.67. In Fig. 2A, RCC-TNFα1 structure harbored a transmembrane region, a TNF domain, seven trimer interface sites ($H^{84}F^{129}Y^{131}Y^{193}F^{198}F^{226}F^{230}$) and six receptor binding sites ($R^{101}K^{102}A^{107}S^{154}S^{161}S^{166}$). In Fig. 2B, secondary structure analysis indicated that RCC-TNFα1 contained 3 sheets, 3 β-hairpins, 3 β-bulges, 5 helices, 12 strands and 1 disulphide. In Fig. 2C, tertiary structure of RCC-TNFα1 was 70 % identical to c7dovB template modeled with exceeding a 95 % confidence.

3.2. Expression profiles of TNFα1 mRNA

In Fig. 3A, tissue-specific TNFα1 mRNA expressions were detected in all isolated samples. The highest expression level of RCC-TNFα1 was observed in gill, whereas the low-level mRNA expression of RCC-TNFα1 was measured in brain.

In Fig. 3B, liver RCC-TNFα1 expression gradually increased from 6 h to 24 h and peaked at 24 h after *A. hydrophila* challenge ($P < 0.05$), followed by a sharp decrease at 48 h. In Fig. 3C, RCC-TNFα1 expression in kidney began to elevated at 6 h and attained the highest level at 48 h after *A. hydrophila* challenge ($P < 0.05$). In Fig. 3D, splenic RCC-TNFα1 expression achieved the peaked level at 48 h following *A. hydrophila* infection ($P < 0.05$).

In addition, LPS is a heat-stable endotoxin of gram-negative pathogens that can exhibit *in vitro* and *in vivo* effect on various immune responses and biological efforts [29]. In our pervious study, we have demonstrated that LPS treatment can induce oxidative stress in RCCFCs, which can be alleviated by administration of *N*-Acetyl-L-cysteine (NAC) [30]. In Fig. 3E, RCCFCs receiving the exposure to 500 ng/mL LPS exhibited elevated expression levels of RCC-TNFα1 mRNA and peaked at 24 h post-stimulation ($P < 0.05$).

3.3. Prokaryotic expression and fusion protein validation

In Fig. 4, a clear IPTG-induced fusion protein band were observed in pET32a-RCC-TNFα1transformed cells in comparison with that of pET32a transformed cells. After Ni-NTA purification, the purified TNFα1 fusion proteins were confirmed by western blotting using anti-His antibody.

3.4. Effect of TNFα1 stimulation on histological changes in midgut

In Fig. 5A and B, RCC anally intubated with RCC-TNFα1 fusion protein exhibited a fuzzy appearance of brush broader in impaired villi along with fusion and edema of midgut wall by comparing with that of the control. In Fig. 5C and D, the average GC numbers reduced sharply and reached a 2.07-fold reduction in villi of RCC-TNFα1 treated midgut in comparison with those of the control ($P < 0.05$), while no significant difference was observed in L/W ratio in midgut villi. In Fig. 5E, a 4.42-fold increase of DAO activity was observed in midgut of RCC subjected to RCC-TNFα1 perfusion.

3.5. Effect of TNFα1 stimulation on immune-related gene expression in midgut

As shown in Fig. 6A, a 1.81-, 1.42-, 1.75-, 2.38-, 1.64-, 3.33-, 5.01- and 1.41-fold decreased expression of ZO-1, claudin 3, claudin 6, claudin 9, occludin, MUC2, MUC7 and MUC13 was observed in midgut following RCC-TNFα1 stimulation. In Fig. 6B and C, relative expressions of FADD, CASP3, CASP7, CASP8, ATF4, ATF6, IRE1, PDIA3 and XBP1 in TNFα1-treated TNFα1 were approximately 4.62-, 4.22-, 2.71-, 5.13-, 3.06-, 2.36-, 3.39-, 6.28- and 2.88-fold greater than those of the control.

3.6. Measurement of antioxidant status in midgut

As shown in Fig. 7A, fish receiving RCC-TNFα1 perfusion exhibited a sharp decrease of HSP70, HSP90α, HSP90β, OXR1, TrxR and SOD1 expression in midgut. In Fig. 7B–E, CAT activity, GPx activity, total SOD

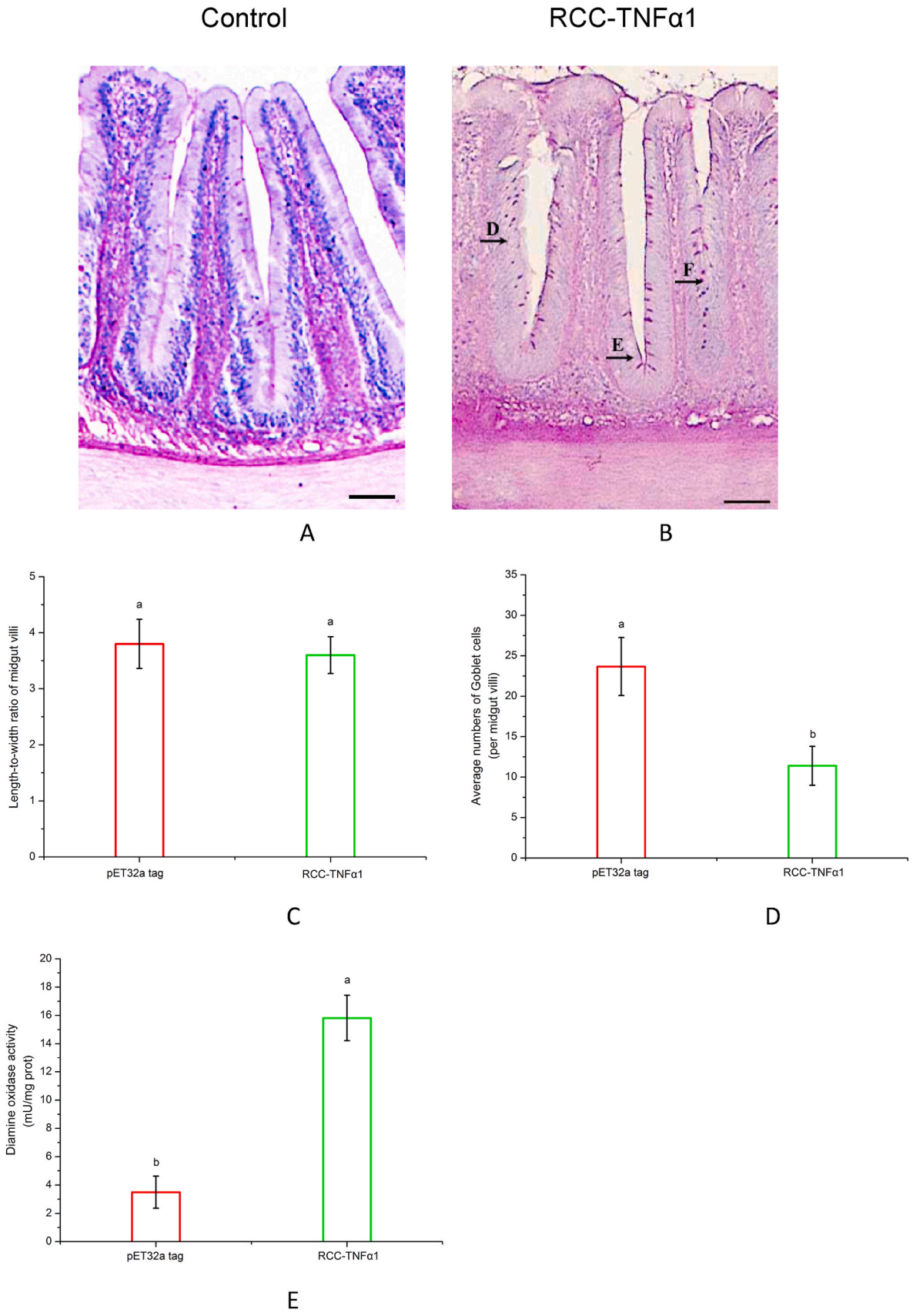

Fig. 5. Histological analysis in midgut by *In vivo* administration of RCC-TNFα1 fusion protein. (A–B) Midgut tissues were sectioned and stained by using PAS staining kit. D: villi deformation; F: villus fusion; E: edema of midgut wall. Villus length-to-width (L/W) ratios (C), average numbers of goblet cells (D) and midgut DAO activities (E) were determined. The calculated data (mean ± SD) with different letters were significantly different ($P < 0.05$) among the groups. The experiments were performed in triplicate.

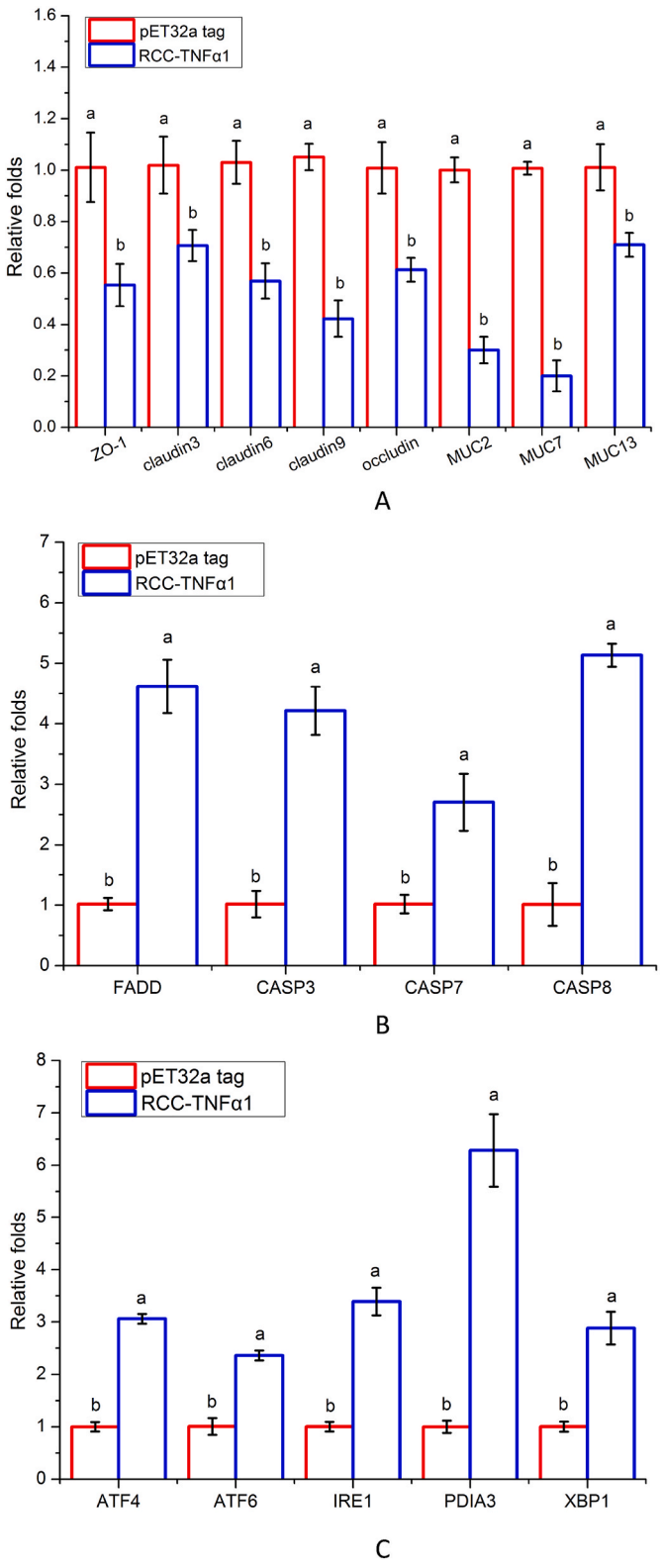

Fig. 6. *In vivo* administration of RCC-TNFα1 fusion protein regulated immune response in midgut. (A) Expressions of TJ genes and mucins in midgut perfused with RCC-TNFα1. (B) Expressions of apoptosis genes in midgut perfused with RCC-TNFα1. (C) Expressions of UPR genes in midgut perfused with RCC-TNFα1. The calculated data (mean ± SD) with different letters were significantly different ($P < 0.05$) among the groups. The experiments were performed in triplicate.

activity and SDH activity decreased dramatically in midgut treated with RCC-TNFα1, while NADPH/$NADP^+$ ratio, ROS content and MDA amount in RCC-TNFα1 group were approximately 3.53-, 3.62- and 2.89-fold greater than those of the control (Fig. 7F–H).

4. Discussion

According to previous transcriptome sequencing data [31], RCC-TNFα1 gene was identified in this study. The deduced RCC-TNFα1 sequence possessed a TNF domain with trimer interface sites and receptor binding sites at highly conserved level, which may generate a compact jellyroll folding. Previous study suggested that efficient signaling transduction of TNF pathways appear to require trimer molecules and receptor binding subunits [32]. These results speculated that RCC-TNFα1 possessing TNF motifs may be functionally conserved. qRT-PCR analysis revealed that RCC-TNFα1 was expressed in a wide range of isolated tissues with a high-expressed level in gill. RCC-TNFα1 expression showed an upregulated trend in liver, kidney and spleen following *A. hydrophila* infection. In addition, similar trend of RCC-TNFα1 expression was observed in RCCFCs following LPS exposure. These results suggested that RCC-TNFα1 may participate in immune response to bacterial invasion. However, the regulatory role of RCC -TNFα1 in gut immunity of fish is unclear.

In general, tight junction integrity serving as physiological barrier plays a crucial role in the front line of innate immune defense against infectious agents in environment [33], while epithelial cells are key sensors of invading microbes that can recruit and chemoattract the adhesion of active immune cells in gut tract [34]. In addition, mucus layer and goblet cells can promote mucosal immune defense against invasive pathogens and facilitate immune cell communication by secreting mucin glycoproteins and bioactive molecules [35,36]. Thus, emerging evidences demonstrate that villi deformation and DAO amount can act as the symptom indicators of mucosal injury in gut tract [37]. Current results indicated that severe pathological symptoms were observed in midgut of RCC perfused with RCC-TNFα1, along with GC reduction and DAO elevation. In addition, expression levels of ZO-1, occludin, claudin 3, claudin 6, claudin 9, MUC2, MUC7 and MUC13 decreased sharply in midgut of RCC following RCC-TNFα1 treatment, suggesting that RCC-TNFα1 treatment could significantly promote epithelial permeability enhance midgut injury in RCC.

As well known, TNFα is one of pivotal ligands in TNF superfamily, which can recruit downstream adaptor protein FADD via TNFα receptor (TNFR) [38]. FADD is a critical component involved in death receptor-mediated extrinsic apoptosis and necroptosis, which can directly determined cell life and death by bridging activated TNFR trimers with CASP signalings [39]. Then, CASP8 activation can orchestrate the execution of extrinsic apoptosis [40]. Programmed cell death, including apoptosis, necrosis and necroptosis, is highly regulated cell death process in immune homeostasis that can elevate immunological tolerance within the host and remodel inflammation in injured tissues [41,42]. Additionally, ROS induced by a variety of stimulators such as TNFα or oxidants can act as a crucial signal molecule and play a pivotal role in the orchestration of innate immunity towards adaptive immune response, but is long-term elevation can impair macromolecular properties [43,44]. HSPs belong to a family of highly conserved chaperones involved in various cellular processes such as protein folding, degradation and translocation, which can serve as stress sensors to regulate host tolerance of oxidative stress and protect against apoptosis [45,46]. OXR1, TrxR, SOD, GPx and CAT can participate in antioxidant defense in response to stimuli [47]. Although antioxidant enzymes and compounds can alleviate cytokine-mediated toxicity, free radical accumulation can exacerbate antioxidant insult and facilitate cell death via caspase signals [48]. Free radical accumulation can also disturb cellular homeostasis, which may enable mounting production of misfolded proteins accumulated in endoplasmic reticulum (ER) to disorder the redox-dependent protein folding process in gut tract [49,50]. However, activated UPR

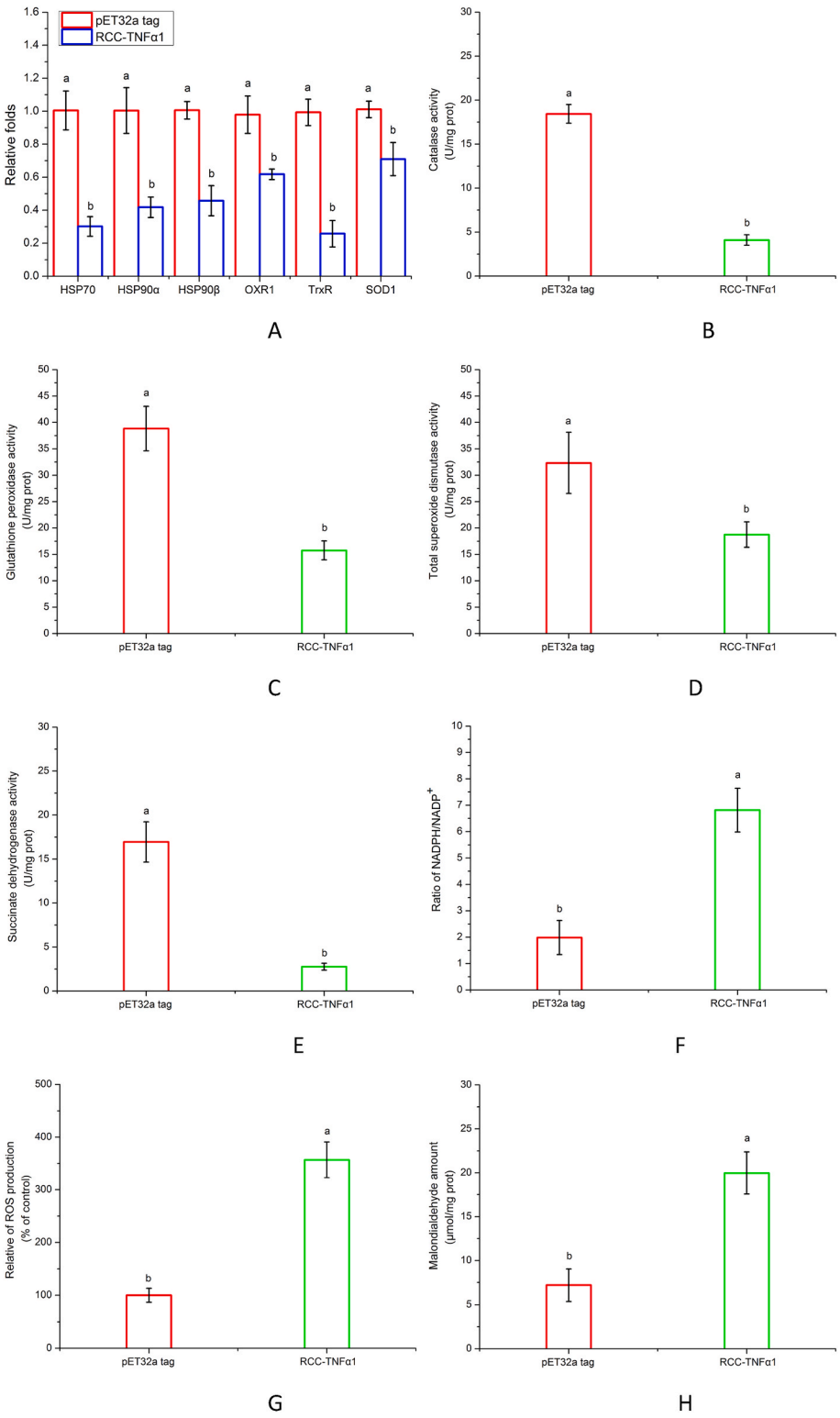

Fig. 7. Effect of RCC-TNFα1 on antioxidant status in midgut. (A) Expressions of antioxidant genes in midgut perfused with RCC-TNFα1. (B–E) Analyses of CAT, GPx, total SOD and SDH were detected in midgut. (F–H) NADPH/$NADP^+$ ratio, relative ROS production and MDA amount were determined in midgut. The calculated data (mean ± SD) with different letters were significantly different ($P < 0.05$) among the groups. The experiments were performed in triplicate.

molecules exert the cytoprotective effort on restoration of cellular homeostasis in tissues or cells suffering from deleterious stressors and severe illness, whereas its subversion enables the collapse of host immune surveillance [51]. In this study, RCC-TNFα1 treatment could attenuate expression profiles of HSP70, HSP90, HSP90β, OXR1, TrxR and SOD1 in midgut of RCC, while the expressions of apoptotic genes and UPR genes increased sharply. In addition, enzymatic activity of CAT, GPx, total SOD and SDH decreased significantly in TNFα1-perfused midgut, along with increased levels of NADPH/$NADP^+$ ratios, ROS production and MDA amount. These results indicated that ROS-induced cytotoxic stress was involved in antioxidant insult and apoptotic activation in TNFα1-treated midgut of RCC.

In conclusion, we characterized the architectures of RCC-TNFα1 for the first time. Expression patterns of RCC-TNFα1 in healthy RCC, *A. hydrophila*-infected RCC and LPS-stimulated cells were measured, respectively. RCC-TNFα1 fusion protein was produced *in vitro*. Gut perfusion with RCC-TNFα1 could significantly impair tight junction function and decrease GC numbers in midgut villi. In addition, RCC-TNFα1 treatment can dramatically decrease antioxidant defense and increase apoptosis in midgut of RCC. Our results revealed that the cytotoxicity of RCC-TNFα1 stimulation may cause the collapse of antioxidant capacity and promote apoptotic process in midgut of RCC.

Ethical approval

All applicable international, national, and/or institutional guidelines for the case and use of animals were followed. Chinese animal welfare laws, guidelines and policies (GB/T 35892–2018).

Completing interests

The authors declare that they have no conflict of interest.

Funding

This research was supported by the National Natural Science Foundation of China, China (grant no. 31902363), Hunan Provincial Natural Science Foundation of China, China (grant no.2021JJ40340).

CRediT authorship contribution statement

Jin-Fang Huang: Methodology. **Ning-Xia Xiong:** Methodology. **Shi-Yun Li:** Formal analysis. **Ke-Xin Li:** Formal analysis. **Jie Ou:** Validation. **Fei Wang:** Validation. **Sheng-Wei Luo:** Conceptualization, Funding acquisition, Writing – original draft, Writing – review & editing.

Declaration of competing interest

The authors declare that they have no conflict of interest.

References

[1] S.S. Killen, S. Marras, N.B. Metcalfe, D.J. McKenzie, P. Domenici, Environmental stressors alter relationships between physiology and behaviour, Trends Ecol. Evol. 28 (2013) 651–658.
[2] B. Magnadottir, Immunological control of fish diseases, Mar. Biotechnol. 12 (2010) 361–379.
[3] S.A. Kraemer, A. Ramachandran, G.G. Perron, Antibiotic pollution in the environment: from microbial ecology to public policy, Microorganisms 7 (2019) 180.
[4] S. Boltaña, N. Roher, F.W. Goetz, S.A. MacKenzie, PAMPs, PRRs and the genomics of gram negative bacterial recognition in fish, Dev. Comp. Immunol. 35 (2011) 1195–1203.
[5] H. Dong, Y. Chen, J. Wang, Y. Zhang, P. Zhang, X. Li, et al., Interactions of microplastics and antibiotic resistance genes and their effects on the aquaculture environments, J. Hazard Mater. (2020), 123961.
[6] Z. Lian, J. Bai, X. Hu, A. Lü, J. Sun, Y. Guo, et al., Detection and characterization of Aeromonas salmonicida subsp. salmonicida infection in crucian carp Carassius auratus, Vet. Res. Commun. 44 (2020) 61–72.
[7] S.T. Oliveira, G. Veneroni-Gouveia, M.M. Costa, Molecular characterization of virulence factors in Aeromonas hydrophila obtained from fish, Pesqui. Vet. Bras. 32 (2012) 701–706.
[8] F. Wang, Z.-L. Qin, W.-S. Luo, N.-X. Xiong, S.-W. Luo, Aeromonas hydrophila can modulate synchronization of immune response in gut-liver axis of red crucian carp via the breach of gut barrier, Aquacult. Int. (2023) 1–15.
[9] J.B. Jørgensen, The innate immune response in fish, Fish Vacc. 1 (2014) 84–102.
[10] I. Salinas, The mucosal immune system of teleost fish, Biology 4 (2015) 525–539.
[11] S. Torrecillas, D. Montero, M.J. Caballero, K.A. Pittman, M. Custódio, A. Campo, et al., Dietary mannan oligosaccharides: counteracting the side effects of soybean meal oil inclusion on European sea bass (Dicentrarchus labrax) gut health and skin mucosa mucus production? Front. Immunol. 6 (2015) 397.
[12] Y. Deng, Y. Zhang, H. Chen, L. Xu, Q. Wang, J. Feng, Gut–liver immune response and gut microbiota profiling reveal the pathogenic mechanisms of vibrio harveyi in pearl gentian grouper (Epinephelus lanceolatus♂× E. fuscoguttatus♀), Front. Immunol. 11 (2020), 607754.
[13] N. Wu, Y.-L. Song, B. Wang, X.-Y. Zhang, X.-J. Zhang, Y.-L. Wang, et al., Fish gut-liver immunity during homeostasis or inflammation revealed by integrative transcriptome and proteome studies, Sci. Rep. 6 (2016) 1–17.
[14] J. Shan, G. Wang, H. Li, X. Zhao, W. Ye, L. Su, et al., The immunoregulatory role of fish specific type II SOCS via inhibiting metaflammation in the gut-liver axis, Water Biol. Syst. 2 (2023), 100131.
[15] H. Himmerich, A.J. Sheldrick, TNF-α and ghrelin: opposite effects on immune system, metabolism and mental health, Protein Pept. Lett. 17 (2010) 186–196.
[16] Y. Li, T. Xiao, J. Zou, Fish TNF and TNF receptors, Sci. China Life Sci. 64 (2021) 196–220.
[17] M. Huang, P. Mu, X. Li, Q. Ren, X.-Y. Zhang, Y. Mu, et al., Functions of TNF-α1 and TNF-α2 in large yellow croaker (Larimichthys crocea) in monocyte/macrophage activation, Dev. Comp. Immunol. 105 (2020), 103576.
[18] S. Kinoshita, G. Biswas, T. Kono, J. Hikima, M. Sakai, Presence of two tumor necrosis factor (tnf)-α homologs on different chromosomes of zebrafish (Danio rerio) and medaka (Oryzias latipes), Mar. Genomics 13 (2014) 1–9.
[19] N.-X. Xiong, Z.-X. Fang, X.-Y. Kuang, J. Ou, S.-W. Luo, S.-J. Liu, Integrated analysis of gene expressions and metabolite features unravel immunometabolic interplay in hybrid fish (Carassius cuvieri♀× Carassius auratus red var♂) infected with Aeromonas hydrophila, Aquaculture 563 (2023), 738981.
[20] S.-W. Luo, Z.-W. Mao, Z.-Y. Luo, N.-X. Xiong, K.-K. Luo, S.-J. Liu, et al., Chimeric ferritin H in hybrid crucian carp exhibit a similar down-regulation in lipopolysaccharide-induced NF-κB inflammatory signal in comparison with Carassius cuvieri and Carassius auratus red var, Comp. Biochem. Physiol. C Toxicol. Pharmacol. 241 (2021) 108966.
[21] C. Fierro-Castro, L. Barrioluengo, P. López-Fierro, B. Razquin, A. Villena, Fish cell cultures as in vitro models of inflammatory responses elicited by immunostimulants. Expression of regulatory genes of the innate immune response, Fish Shellfish Immunol. 35 (2013) 979–987.
[22] G.-H. Cha, S.-W. Luo, Z-h Qi, Y. Liu, W.-N. Wang, Optimal conditions for expressing a complement component 3b functional fragment (α2-macroglobulin receptor) gene from Epinephelus coioides in Pichia pastoris, Protein Express Purif 109 (2015) 23–28.
[23] C.-H. Cheng, F.-F. Yang, S.-A. Liao, Y.-T. Miao, C.-X. Ye, A.-L. Wang, et al., Identification, characterization and functional analysis of anti-apoptotic protein BCL-2-like gene from pufferfish, Takifugu obscurus, responding to bacterial challenge, Fish Physiol. Biochem. 41 (2015) 1053–1064.
[24] X. Song, J. Zhao, Y. Bo, Z. Liu, K. Wu, C. Gong, Aeromonas hydrophila induces intestinal inflammation in grass carp (Ctenopharyngodon idella): an experimental model, Aquaculture 434 (2014) 171–178.
[25] J. Ou, W.-S. Luo, Z.-R. Zhong, Q. Xie, F. Wang, N.-X. Xiong, et al., Manganese-superoxide dismutase (MnSOD) rescues redox balance and mucosal barrier function in midgut of hybrid fish (Carassius cuvieri♀× Carassius auratus red var♂) infected with Aeromonas hydrophila and Edwardsiella tarda, Reprod. Breed. 3 (2023) 108–117.
[26] N.-X. Xiong, F. Wang, W.-S. Luo, J. Ou, Z.-L. Qin, M.-Z. Huang, et al., Tumor necrosis factor α2 (TNFα2) facilitates gut barrier breach by Aeromonas hydrophila and exacerbates liver injury in hybrid fish, Aquaculture 577 (2023) 739995.
[27] C.-H. Cheng, Y.-L. Su, H.-L. Ma, Y.-Q. Deng, J. Feng, X.-L. Chen, et al., Effect of nitrite exposure on oxidative stress, DNA damage and apoptosis in mud crab (Scylla paramamosain), Chemosphere 239 (2020), 124668.
[28] M.K. Jeong, B.-H. Kim, Grading criteria of histopathological evaluation in BCOP assay by various staining methods, Toxicol. Res. 38 (2022) 9–17.
[29] W. Lee, E.-J. Yang, S.-K. Ku, K.-S. Song, J.-S. Bae, Anti-inflammatory effects of oleanolic acid on LPS-induced inflammation in vitro and in vivo, Inflammation 36 (2013) 94–102.
[30] S.-W. Luo, N.-X. Xiong, Z.-Y. Luo, K.-K. Luo, S.-J. Liu, C. Wu, et al., Effect of Lipopolysaccharide (LPS) stimulation on apoptotic process and oxidative stress in fibroblast cell of hybrid crucian carp compared with those of Carassius cuvieri and Carassius auratus red var, Comp. Biochem. Physiol. C Toxicol. Pharmacol. 248 (2021), 109085.
[31] N.-X. Xiong, J. Ou, L.-F. Fan, X.-Y. Kuang, Z.-X. Fang, S.-W. Luo, et al., Blood cell characterization and transcriptome analysis reveal distinct immune response and host resistance of different ploidy cyprinid fish following Aeromonas hydrophila infection, Fish Shellfish Immunol. 120 (2022) 547–559.
[32] É.S. Vanamee, D.L. Faustman, Structural principles of tumor necrosis factor superfamily signaling, Sci. Signal. 11 (2018), eaao4910.
[33] E.E. Schneeberger, R.D. Lynch, The tight junction: a multifunctional complex, Am. J. Physiol. Cell Physiol. 286 (2004) C1213–C1228.
[34] M.F. Kagnoff, L. Eckmann, Epithelial cells as sensors for microbial infection, J. Clin. Invest. 100 (1997) 6–10.
[35] Y.S. Kim, S.B. Ho, Intestinal goblet cells and mucins in health and disease: recent insights and progress, Curr. Gastroenterol. Rep. 12 (2010) 319–330.
[36] T. Pelaseyed, J.H. Bergström, J.K. Gustafsson, A. Ermund, G.M. Birchenough, A. Schütte, et al., The mucus and mucins of the goblet cells and enterocytes provide the first defense line of the gastrointestinal tract and interact with the immune system, Immunol. Rev. 260 (2014) 8–20.
[37] J-j Zhang, J-q Wang, X-y Xu, J-y Yang, Z. Wang, S. Jiang, et al., Red ginseng protects against cisplatin-induced intestinal toxicity by inhibiting apoptosis and autophagy via the PI3K/AKT and MAPK signaling pathways, Food Funct. 11 (2020) 4236–4248.
[38] B. Beutler, C. Van Huffel, Unraveling function in the TNF ligand and receptor families, Science 264 (1994) 667–668.
[39] L. Tourneur, G. Chiocchia, FADD: a regulator of life and death, Trends Immunol. 31 (2010) 260–269.

[40] H.-B. Shu, D.R. Halpin, D.V. Goeddel, Casper is a FADD-and caspase-related inducer of apoptosis, Immunity 6 (1997) 751–763.
[41] C. Günther, H. Neumann, M.F. Neurath, C. Becker, Apoptosis, necrosis and necroptosis: cell death regulation in the intestinal epithelium, Gut 62 (2013) 1062–1071.
[42] M. Chen, Y.-H. Wang, Y. Wang, L. Huang, H. Sandoval, Y.-J. Liu, et al., Dendritic cell apoptosis in the maintenance of immune tolerance, Science 311 (2006) 1160–1164.
[43] K. Kaur, A.K. Sharma, S. Dhingra, P.K. Singal, Interplay of TNF-α and IL-10 in regulating oxidative stress in isolated adult cardiac myocytes, J. Mol. Cell. Cardiol. 41 (2006) 1023–1030.
[44] Y.J. Suzuki, H.J. Forman, A. Sevanian, Oxidants as stimulators of signal transduction, Free Radic. Biol. Med. 22 (1997) 269–285.
[45] E. Padmini, M. Usha Rani, Heat-shock protein 90 alpha (HSP90α) modulates signaling pathways towards tolerance of oxidative stress and enhanced survival of hepatocytes of Mugil cephalus, Cell Stress Chaperones 16 (2011) 411–425.
[46] M.A. Yenari, J. Liu, Z. Zheng, Z.S. Vexler, J.E. Lee, R.G. Giffard, Antiapoptotic and anti-inflammatory mechanisms of heat-shock protein protection, Ann. N. Y. Acad. Sci. 1053 (2005) 74–83.
[47] A. Sahreen, K. Fatima, T. Zainab, M.K. Saifullah, Changes in the level of oxidative stress markers in Indian catfish (Wallago attu) infected with Isoparorchis hypselobagri, Beni-Suef Univ. J. Basic Appl. Sci. 10 (2021) 1–8.
[48] MalikAsrarReactive oxygen species in inflammation and tissue injury, Antioxidants Redox Signal 14 (2020) 1126–1167.
[49] A. Bhattacharyya, R. Chattopadhyay, S. Mitra, S.E. Crowe, Oxidative stress: an essential factor in the pathogenesis of gastrointestinal mucosal diseases, Physiol. Rev. 94 (2014) 329–354.
[50] W.C. Chong, M.D. Shastri, R. Eri, Endoplasmic reticulum stress and oxidative stress: a vicious nexus implicated in bowel disease pathophysiology, Int. J. Mol. Sci. 18 (2017) 771.
[51] J. Celli, R.M. Tsolis, Bacteria, the endoplasmic reticulum and the unfolded protein response: friends or foes? Nat. Rev. Microbiol. 13 (2015) 71–82.